ANALYTICAL PERFORMANCE BOUND ON A CORRELATION MATRIX BASED BLIND EQUALIZER

Jukka Mannerkoski and Visa Koivunen*

Signal Processing Laboratory, Tampere University of Technology
P.O. Box 553, FIN-33101 Tampere, Finland
fax: +358-3-365 3857
email: {jhm, visa}@cs.tut.fi

Keywords – communications, blind channel equalization, second-order cyclostationarity.

ABSTRACT

Blind equalizers are used to remove the inter-symbol interference (ISI) caused by a communication channel without knowing the transmitted sequence. Blind equalizers can be obtained from the second-order cyclostationary statistics of the received sequence. The successful equalization of a mixed-phase communication channel often requires a suitable delay at the output of the equalizer. An arbitrary delay blind equalizer can be obtained with the correlation matrix (CM) method of [2]. In this paper, an analytical lower bound for the mean-squared error (MSE) of the CM-equalizer is derived. The MSE is evaluated for example channels and simulations are used to verify the analytical results. For comparison, simulation results obtained with three other algorithms are given. The equalizer performance is studied in simulation as a function of the magnitude of the first channel coefficient.

1. INTRODUCTION

In a communication system, the transmitted signal is convolved with the impulse response of the multi-path propagation channel. Equalization attempts to remove the consequent inter-symbol interference (ISI) from the received sequence of symbols. We focus on blind equalizers that have no access to the transmitted sequence, as opposed to conventional methods that rely on a predetermined training sequence. Fractional sampling resulting in a single-input multiple-output (SIMO) system model is employed.

The mean-squared error (MSE) of the symbol estimate may critically depend on the delay of the equalizer (c.f. [2]). The suitable delay can be linked to the energy concentration of the channel impulse response. Blind equalizers that have control over their delay are, e.g., the direct correlation matrix based (CM) equalizers of [2] and the multi-step prediction-error filter (PEF) based algorithms introduced in [1] and [9]. An analytical lower-bound on the MSE of the PEF-approach was derived in [4] and [5]. It was observed that regardless of the delay, the MSE remains high even for high SNRs if the first coefficient of each subchannel is small in magnitude. The CM- and PEF-approaches are identical for zero-delay equalization [6]. Therefore, it is interesting to investigate whether the dependence on the first channel coefficient of the PEF-equalizers carries over to the CM-equalizer for other delays as well.

In this paper, we derive an analytical lower bound for the MSE of the CM-equalizer of arbitrary delay as a function of the channel impulse response and the SNR. The MSE is evaluated for two channels and simulations are used to verify the results. The results are compared to the results obtained by a prediction based FF-PEF algorithm introduced in [1], a subspace based equalizer (SBE) of [7] and a fractionally sampled constant modulus algorithm (FS-CMA) (c.f. [3]). The dependence of the CM-equalizer performance on the magnitude of the first channel coefficient is studied in simulation.

This paper is organized as follows. The system model is presented in section 2. The CM-equalizer is described in section 3 and a lower bound for its MSE is derived. The blind equalizers used in comparison are described in section 4 and the analytical and simulation results are presented in section 5.

2. SYSTEM MODEL

Let $x(k)$ denote the symbol emitted by a random digital source at time kT, T being the symbol period. The channel is considered to be linear and time-invariant (LTI) during a time window sufficient to allow its estimation. The continuous time received signal is

$$y(t) = \sum_{k=-\infty}^{\infty} x(k)h(t-kT) + v(t) \qquad (1)$$

where $h(t)$ is the complex baseband channel impulse response, $x(k)$ is the sequence of complex information symbols and $v(t)$ is additive white noise with variance σ_v^2.

When $P \geq 2$ samples of $y(t)$ per symbol interval are available at the receiver, the system can be modeled as consisting of P subchannels. The ith subchannel response is defined as $h_i(n) \triangleq h(t_0 + iT/P + nT),\ n = 0, \dots, L_h - 1$, where L_h is the subchannel length. Its output sequence $y_i(n) \triangleq y(t_0+iT/P+nT)$ is

$$y_i(n) = \sum_{k=0}^{L_h-1} x(n-k)h_i(k) + v_i(n) \qquad (2)$$

where $i = 0, \dots, P-1$, $-\infty < n < \infty$, $v_i(n)$ are samples of $v(t)$ corresponding to $y_i(n)$ and the symbol period is normalized to $T = 1$. In each symbol interval, a vector $\mathbf{y}(n) = [y_0(n), \dots, y_{P-1}(n)]^T$ of length P is received, $[\,]^T$ denoting transposition. The channel impulse response can also be represented in vector form as $\mathbf{h}(n) = [h_0(n), \dots, h_{P-1}(n)]^T$ and the noise as $\mathbf{v}(n) = [v_0(n), \dots, v_{P-1}(n)]^T$. We consider a finite symbol sequence of length M and define a matrix $\mathcal{H}_M$ with dimension $MP \times (L_h + M - 1)$ consisting of the channel coefficient vectors,

$$\mathcal{H}_M = \begin{bmatrix} \mathbf{h}(0) & \dots & \mathbf{h}(L_h-1) & & \mathbf{0}_{P\times(M-1)} \\ & \ddots & & \ddots & \\ \mathbf{0}_{P\times(M-1)} & & \mathbf{h}(0) & \dots & \mathbf{h}(L_h-1) \end{bmatrix} \qquad (3)$$

Stacking M received vector samples into an $(MP \times 1)$-vector $\mathbf{y}_M(n) = [\mathbf{y}^T(n), \dots, \mathbf{y}^T(n-M+1)]^T$, we can write a matrix

* This work was funded by the Academy of Finland

equation for the system as

$$\mathbf{y}_M(n) = \mathcal{H}_M \mathbf{x}_{L_h+M-1}(n) + \mathbf{v}_M(n) \tag{4}$$

where the input vector is $\mathbf{x}_{L_h+M-1}(n) = [x(n), \ldots, x(n - L_h - M + 2)]^T$ [10].

We denote the correlation matrix of $\mathbf{y}_M(n)$ as

$$\tilde{\mathbf{R}}_M = \mathrm{E}[\mathbf{y}_M(n)\mathbf{y}_M^H(n)] = \mathcal{H}_M \mathcal{H}_M^H + \sigma_v^2 \mathbf{I} \tag{5}$$

When the noise power $\sigma_v^2 = 0$, the correlation matrix is denoted $\mathbf{R}_M = \mathcal{H}_M \mathcal{H}_M^H$. We further define the time-shifted correlation matrices

$$\tilde{\mathbf{R}}_{M,d} = \mathrm{E}[\mathbf{y}_M(n)\mathbf{y}_M^H(n-d)] \tag{6}$$

for the noisy case $\sigma_v^2 \neq 0$ and $\mathbf{R}_{M,d} = \mathrm{E}[\mathbf{y}_M(n)\mathbf{y}_M^H(n-d)]$ for $\sigma_v^2 = 0$. The following assumptions will be used in this paper:

- A1. The input sequence $x(t)$ is zero-mean and white with unit variance.
- A2. The additive noise $v(t)$ is zero-mean and white with variance σ_v^2.
- A3. The sequences $x(t)$ and $v(t)$ are uncorrelated.
- A4. The matrix $\mathcal{H}_M$ has full column rank, i.e. the subchannels $h_i(n)$ have no common zeros.

3. CORRELATION MATRIX BASED BLIND EQUALIZATION

3.1. Zero-forcing equalization

An equalizer with delay d is represented as $\mathbf{g}_d = [\mathbf{g}^T(0), \ldots, \mathbf{g}^T(L_g-1)]^T$, where $\mathbf{g}(n) = [g_0(n), \ldots, g_{P-1}(n)]^T$ and L_g is the equalizer length. Subchannel $h_i(n)$ is equalized with $g_i(n)$ and the symbol estimate consists of the sum of the outputs as

$$\hat{x}(n-d) = \mathbf{g}_d \mathbf{y}_{L_g} \tag{7}$$

as shown in Fig. 1 for $P = 2$.

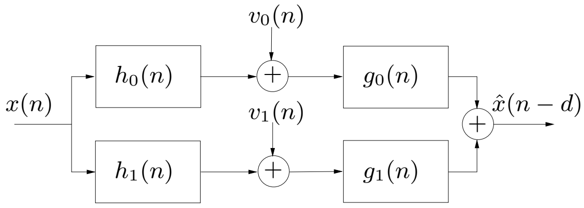

Figure 1: A multichannel communication system.

A zero-forcing (ZF) equalizer retrieves the transmitted symbol without error in the absence of noise. In this paper, we consider a d-delay blind ZF-equalizer derived in [2]. First, a zero-delay equalizer is computed as

$$\mathbf{g}_0 = \mathbf{H}^H(0)\mathbf{R}_{L_g}^{\dagger} \tag{8}$$

where $\mathbf{H}(0)$ is the first column of $\mathcal{H}_{L_g}$ and $\mathbf{R}_{L_g}^{\dagger}$ is the pseudo-inverse of $\mathbf{R}_{L_g}$. The relation between $\mathbf{g}_0$ and $\mathbf{g}_d$ is given by [2]

$$\mathbf{g}_d \mathbf{R}_{L_g} = \mathbf{g}_0 \mathbf{R}_{L_g,d} \tag{9}$$

which results in the d-delay ZF-equalizer

$$\mathbf{g}_d = \mathbf{H}^H(0)\mathbf{R}_{L_g}^{\dagger}\mathbf{R}_{L_g,d}\mathbf{R}_{L_g}^{\dagger} \tag{10}$$

The first channel coefficient $\mathbf{h}(0)$ is assumed to be known. We will not consider its estimation in this paper.

3.2. A performance bound in the presence of noise

In this section, a lower bound on the MSE of the blind zero-forcing CM-equalizer is derived, when additive white noise with an unknown variance σ_v^2 is present in the system. The equalizer is computed by substituting the correlation matrices $\mathbf{R}_{L_g}$ and $\mathbf{R}_{L_g,d}$ in (10) by their noisy counterparts $\tilde{\mathbf{R}}_{L_g}$ and $\tilde{\mathbf{R}}_{L_g,d}$

$$\tilde{\mathbf{g}}_d = \mathbf{H}^H(0)\tilde{\mathbf{R}}_{L_g}^{\dagger}\tilde{\mathbf{R}}_{L_g,d}\tilde{\mathbf{R}}_{L_g}^{\dagger} \tag{11}$$

In addition to the ZF-equalizer $\mathbf{g}_d$, the equalizer $\tilde{\mathbf{g}}_d$ includes an error term

$$\mathbf{g}_d^e = \tilde{\mathbf{g}}_d - \mathbf{g}_d \tag{12}$$

The output of the equalizer is now

$$\begin{aligned}\hat{x}(n-d) &= \tilde{\mathbf{g}}_d \mathbf{y}_{L_g}(n) \\ &= \tilde{\mathbf{g}}_d \mathcal{H}_{L_g}\mathbf{x}_{L_h+L_g-1}(n) + \tilde{\mathbf{g}}_d \mathbf{v}_{L_g}(n) \\ &= x(n-d) + \mathbf{g}_d^e \mathcal{H}_{L_g}\mathbf{x}_{L_h+L_g-1}(n) + \tilde{\mathbf{g}}_d \mathbf{v}_{L_g}(n) \\ &= x(n-d) + \epsilon(n)\end{aligned} \tag{13}$$

where we have defined the estimation error as

$$\epsilon(n) \triangleq \mathbf{g}_d^e \mathcal{H}_{L_g}\mathbf{x}_{L_h+L_g-1}(n) + \tilde{\mathbf{g}}_d \mathbf{v}_{L_g}(n) \tag{14}$$

The latter component of $\epsilon(n)$ is due to the noise colored by the equalizer. The first component is additional interference that stems from the error in computing the equalizer from the noisy correlation matrices. The MSE $J_\epsilon = \mathrm{E}[\epsilon(n)\epsilon^H(n)]$ at the output of the d-delay equalizer is then

$$J_\epsilon = \mathbf{g}_d^e \mathcal{H}_{L_g}\mathcal{H}_{L_g}^H \mathbf{g}_d^{eH} + \sigma_v^2 \tilde{\mathbf{g}}_d \tilde{\mathbf{g}}_d^H \tag{15}$$

4. BLIND ALGORITHMS USED IN COMPARISON

For delay $d = 0$, the CM-equalizer (10) was shown in [6] to be identical to the prediction-error filter (PEF) based equalizer presented in [8]. It is interesting to study whether the prediction-based equalizers behave similarly to the CM-equalizer for arbitrary d. We consider the FF-PEF algorithm, which was originally presented in [1]. It is based on the outputs of two multi-step PEFs. The k-step forward linear PEF of order M produces the prediction error $\mathbf{f}_{M,k}(n)$ at its output. The filter coefficients can be computed with the Wiener-Hopf equations. The symbol estimate is obtained as

$$\hat{x}(n-k) = [\mathbf{h}^H(k)\mathbf{h}(k)/\mathbf{h}^H(k)]\mathbf{F}_{M,k}(n) \tag{16}$$

where $\mathbf{F}_{M,k}(n) = \mathbf{f}_{M,k+1}(n) - \mathbf{f}_{M,k}(n)$. The major visible difference to the CM-equalizer (10) is the FF-PEF dependence on the channel coefficient $\mathbf{h}(k)$ instead of $\mathbf{h}(0)$. The symbol estimate is exact in the absence of noise. Analytical lower bound for the MSE of the FF-PEF in noise is given in [4] and [5].

The second algorithm that is used in the simulations is the subspace-based equalizer of [7], denoted here by SBE. The algorithm exploits the orthogonality property between the signal and noise subspaces of $\tilde{\mathbf{R}}_M$. Eigen-decomposition provides the basis vectors spanning the subspaces. A matrix containing equalizers of various delays can be constructed.

Finally, we use the adaptive FS-CMA algorithm in the simulations (c.f. [3]). Unlike the three other equalizers considered in this paper that use second-order cyclostationary statistics, the FS-CMA is based on higher-order statistics. We are interested in seeing how the FS-CMA performance differs from the performance of the second-order algorithms for a channel with $\mathbf{h}(0)$ small in magnitude. Due to the fractional sampling, the FS-CMA avoids the local minima inherent in the error surface of the symbol-spaced CMA-algorithm. Similarly to the algorithms using second-order CS-statistics, the subchannels are not allowed to have any common zero.

5. ANALYTICAL AND SIMULATED RESULTS

The analytical results derived in section 3.2 are evaluated here for channels 1 and 2, whose impulse response magnitudes are shown in Fig. 2. They are both empirically measured microwave channels obtained from the web-site *http://spib.rice.edu/spib /microwave.html*. Verification of the analytical results and performance of the comparison algorithms is obtained with simulations. The source sequence is white 16-QAM and the additive noise is white and Gaussian. In the simulations, a sample size of 25 000 is used to estimate the correlation matrices. An independent test set of 5000 symbols is used at each evaluated point and the results are averaged over 100 Monte-Carlo runs. The SNR is defined as SNR $:= \mathrm{E}[\Sigma_{j=0}^{P-1}|y_j'(n)|^2/\Sigma_{k=0}^{P-1}|v_k(n)|^2]$ where $y_j'(n)$ is the signal component of $y_j(n)$.

The simulation results confirm the analysis of the CM-algorithm performance, as seen from Fig. 3 for channel 1. The analytical lower bound for the MSE (15) is plotted together with the simulation results of the equalizers. An optimum value for the delay d is used in all the simulations. The results of the CM-equalizer are similar to those of the prediction-based FF-PEF. The FS-CMA has a higher MSE than the CM-equalizer and the FF-PEF for this particular channel and the SBE requires a high SNR to perform well.

In [5], the analytical MSE of the FF-PEF for channel 2 was shown to be high even for high SNRs. From Fig. 4, we can see that also the CM-algorithm has a large error at its output for channel 2, despite the optimum delay $d = 3$. The performance of the CM-equalizer and the FF-PEF are now equal. The dependence of the SBE on the SNR is even more emphasized than for channel 1. For moderate SNRs, the FS-CMA has a MSE of almost two orders of magnitude smaller than the methods based on second-order statistics.

The MSE at the output of channel 2 is large compared to the error at the output of channel 1. The reason is the small magnitude of the first coefficient $\mathbf{h}(0)$ of channel 2. We demonstrate this by evaluating the error (15) for random channels of length $8T$. The uncorrelated channel tap coefficients are drawn from a complex Gaussian distribution with zero mean and unit variance, resulting in a Rayleigh distribution for the magnitude of each tap. The total error and its components are plotted in Fig. 5 as a function of the relative magnitude of $\mathbf{h}(0)$ to the magnitude of the entire channel, defined as

$$M[\mathbf{h}(0)] \triangleq \frac{|h_0(0)| + |h_1(0)|}{\sum_{i=0}^{L_h-1}\{|h_0(i)| + |h_1(i)|\}} \times 100\%$$

At each evaluated point, $M[\mathbf{h}(0)] = 2, \ldots, 25\%$, the results are averaged over at least 1000 realizations of the random channel. The SNR is 30 dB and the delay resulting in the smallest total MSE was chosen for each realization of the random channel. The interference component is the dominating error source at small values of $M[\mathbf{h}(0)]$. The MSE decreases as the magnitude of the first channel coefficient vector $\mathbf{h}(0)$ increases, which is the same observation that was made for the PEF-based equalizers in [5]. The average condition number of $\mathcal{H}_M$ is also plotted to show that the large MSE at low values of $M[\mathbf{h}(0)]$ is not due to the violation of assumption A4, i.e. the rank of $\mathcal{H}_M$ is not affected by $M[\mathbf{h}(0)]$. Fig. 6 shows the results of the same experiment as a function of the channel coefficient $\mathbf{h}(1)$. The interference component is now consistently larger than the colored noise, but the $M[\mathbf{h}(1)]$ does not affect the average performance of the CM-equalizer. This indicates that the critical factor is indeed the magnitude of $\mathbf{h}(0)$.

Because the majority of the MSE for channel 2 is due to the interference component in (15), it would be tempting to set the $\mathbf{g}_d^e$ to zero by using the noiseless correlation matrices $\mathbf{R}_{L_g}$ and $\mathbf{R}_{L_g,d}$ in (11). This can be done if the noise power σ_v^2 is known. However, the rank-deficiency of the matrix $\mathbf{R}_{L_g}$ causes problems in the computation of the equalizer. For analytical results that are computed from the exact statistics, the method results in performance improvement at high SNRs, as seen from Fig. 7. For the realistic situation with sample statistics, the results degrade when the noise component is removed from the correlation matrices.

6. CONCLUSIONS

A lower bound for the direct blind CM-equalizer of [2] was derived. The MSE of the equalizer was evaluated for example channels and verified with simulations. The performance was observed to depend heavily on the magnitude of the first channel coefficient $\mathbf{h}(0)$. It was also noted that the dependence was not due to the rank variations in the channel matrix $\mathcal{H}_M$. It is well known that an appropriate delay at the output of the equalizer is often required to ensure a small MSE when the communication channel is mixed-phase. Our results indicate that the delay alone is not sufficient to guarantee a good performance. A large MSE may result even at high SNRs when the $\mathbf{h}(0)$ is small in magnitude.

The performance of the SBE is poor for channel 2 until high SNRs, where it improves significantly. This suggests that a small magnitude of $\mathbf{h}(0)$ affects the signal and noise subspaces in such a way that the acquisition of the equalizers from the correlation matrix becomes a difficult task. The performance of the FS-CMA is not sensitive to the magnitude of the $\mathbf{h}(0)$, unlike the second-order statistics based equalizers considered in this paper. An interesting future research topic is which other second-order methods behave similarly to this type of channels.

7. REFERENCES

[1] D. Gesbert and P. Duhamel. Robust blind channel identification and equalization based on multi-step predictors. In *Proc. of ICASSP'97*, pages 3621–3624, 1997.

[2] G. B. Giannakis and S. D. Halford. Blind fractionally spaced equalization of noisy FIR channels: Direct and adaptive solutions. *IEEE Trans. Signal Proc.*, 45(9):2277–2292, September 1997.

[3] Y. Li and Z. Ding. Global convergence of fractionally-spaced godard (CMA) adaptive equalizers. *IEEE Trans. Signal Proc.*, 44(4), April 1996.

[4] J. Mannerkoski and V. Koivunen. Error analysis of a multi-step prediction based blind equalizer. Submitted for publication, *ISCAS'99*.

[5] J. Mannerkoski and V. Koivunen. Performance bounds for multi-step prediction based blind equalization. *IEEE Trans. Comm.*, submitted for publication 1998.

[6] J. Mannerkoski and D. P. Taylor. Blind equalization using least-squares lattice prediction. *IEEE Trans. Signal Proc.*, to appear, 1998.

[7] E. Moulines, P. Duhamel, J.-F. Cardoso, and S. Mayrargue. Subspace methods for the blind identification of multichannel FIR filters. *IEEE Trans. Signal Proc.*, 43(2):516–525, February 1995.

[8] D. T. Slock. Blind fractionally-spaced equalization, perfect reconstruction filter banks and multichannel linear prediction. In *Proc. of ICASSP'94*, pages IV585–IV588, Adelaide, Australia, April 1994.

[9] D. T. Slock and C. B. Papadias. Further results on blind identification and equalization of multiple FIR channels. In *Proc. of ICASSP'95*, pages 1964–1967, Detroit, MI, May 1995.

[10] L. Tong, G. Xu, and T. Kailath. Blind identification based on second-order statistics: A frequency-domain approach. *IEEE Trans. Info. Theory*, 41(1):329–334, January 1995.

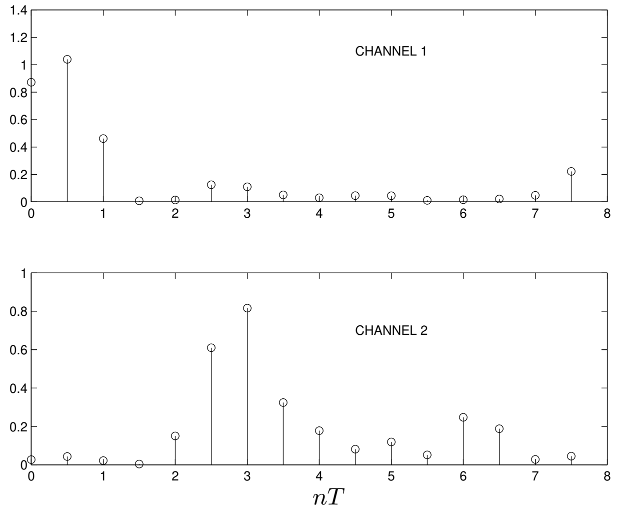

Figure 2: Magnitude of channels 1 and 2.

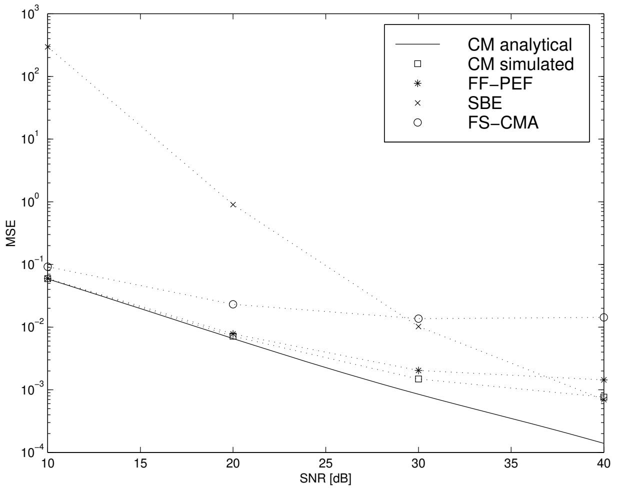

Figure 3: MSE of the blind equalizer output, $d = 1$, channel 1.

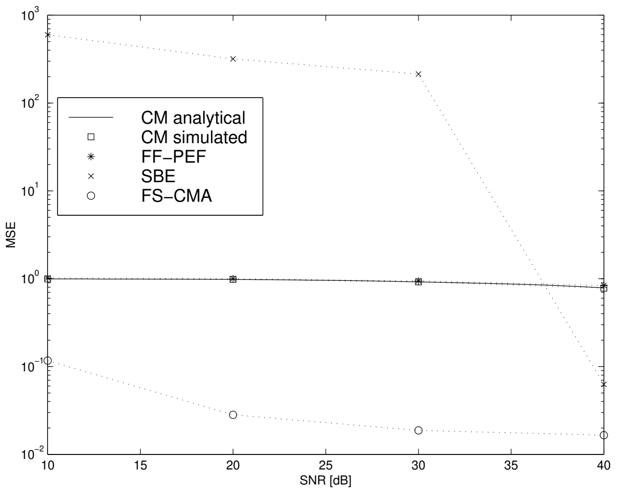

Figure 4: MSE of the blind equalizer output, $d = 3$, channel 2.

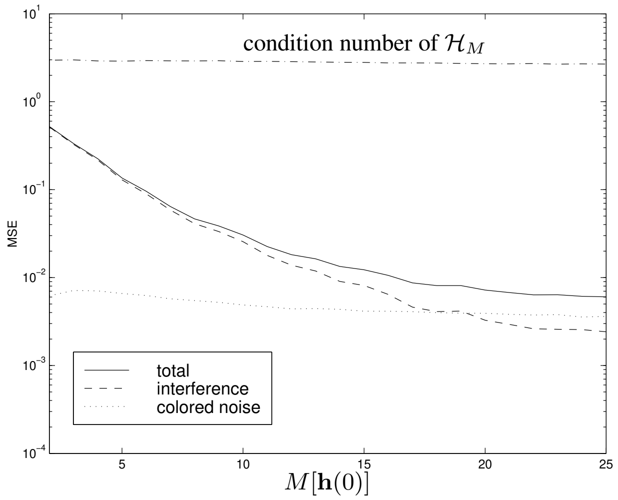

Figure 5: Error dependence on the relative $\mathbf{h}(0)$ magnitude, random channels, SNR of 30 dB.

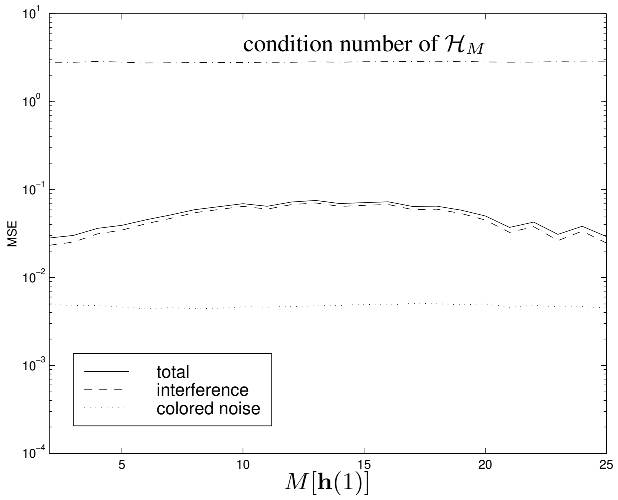

Figure 6: Error dependence on the relative $\mathbf{h}(1)$ magnitude, random channels, SNR of 30 dB.

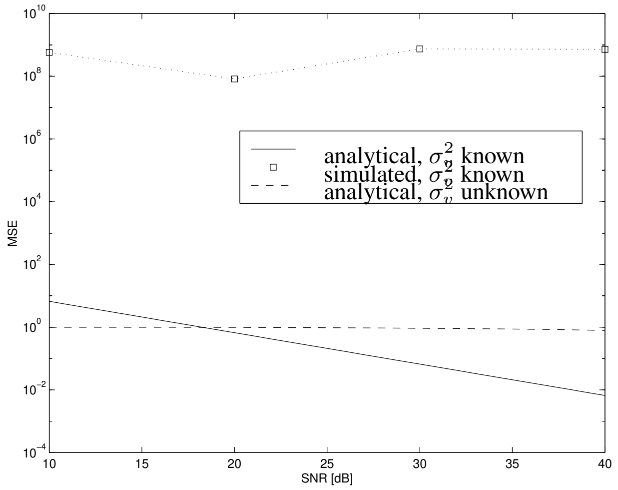

Figure 7: Performance of the CM-equalizer, when σ_v^2 is known.